Comparisons of numerical modelling of the Selective Laser Melting

Laurent van Belle, Guillaume Vansteenkiste, Jean-Claude Boyer

Key Engineering Materials Vols. 504-506 (2012) pp 1067-1072
Online available since 2012/Feb/03 at www.scientific.net

doi:10.4028/www.scientific.net/KEM.504-506.1067

Comparisons of numerical modelling of the Selective Laser Melting

Laurent VAN BELLE[1, 2, a], Guillaume VANSTEENKISTE[2, b]

Jean-Claude BOYER[1, c]

[1]Laboratoire de Mécanique des Contacts et des Structures, INSA de Lyon

20 avenue A. Einstein, 69100 Villeurbanne, Université de Lyon, France

[2]Business Unit Processes & Tools, PEP : Centre technique de la plasturgie,

2 rue P. et M. Curie, 01100 Bellignat, France

[a]laurent.van-belle@insa-lyon.fr, [b]guillaume.vansteenkiste@poleplasturgie.com

[c]jean-claude.boyer@insa-lyon.fr

Keywords: Selective laser melting, Thermomechanical simulation, Residual stresses.

Abstract. Selective laser melting (SLM) first developed for rapid prototyping (RP) is now used for rapid manufacturing of parts with inner complex shapes that cannot be made by more conventional routes. For example, production of injection moulds with cooling channels is of special interest.

In this paper, a numerical model of SLM process was investigated to simulate the genesis of residual stresses. The proposed numerical modelling is based upon a double meshing with a multi step birth and death technique of manufactured part. The influence of the mesh size is analysed with element as small as the powder layer thickness for 2D and 3D geometries of simple parts. Comparisons between plane stress, plane strain, and 3D analysis are presented in order to propose a simplified approach.

Introduction

As a first step, Rapid Prototyping was used to create prototypes from CAD for communication and inspection purposes in a short time, whereas nowadays Rapid Tooling (RT) is used to manufacture directly and quickly end-use parts with complex shapes. Warm and arc additive layer manufacturing (WAALM), laser metal deposition (LMD), selective laser melting (SLM), etc., are emerging technologies allowing manufacturing in a single step parts from their 3D CAD models. The main benefits of the Rapid Manufacturing are its ability to create complex internal geometry impossible to obtain with other classical techniques, and the reduction of design process [1]. This paper deals only with the selective laser melting (SLM) process where the part is first cut numerically into thin slices to get a multilayered CAD model. Then, each metallic powder layer is successively laid down on a horizontal bed-plate and converted in a sound material by melting with a high intensity laser beam on the previous solidified layers. The path of the laser beam is controlled in agreement with the cross-sections generated from the 3D CAD model (Fig. 1). The material density of the manufactured parts is close to the density of molded parts. For example, this process is very versatile to produce steel injection moulds with internal cooling channels.

The laser beam generates heating cycles in the vicinity of its radiation, so violent cooling takes place with strong temperature gradients in the solidified layer. As cyclic thermal expansions and contractions far exceed the maximum elastic strain of the material, heterogeneous plastic strains are cumulated in the manufactured part generating internal stresses. Their level can reach the strength of the material and cracks may appear during the process or reduce the fatigue life of the part, so it is necessary to analyze the genesis of the residual stress in order to reduce them. Residual stresses have been investigated with experimental methods like the hole drilling technique presented in [2]. The bridge curvature technique presented in [3] and the layer removal technique presented in [4] are also used to analyze the residual stress distributions in metallic parts manufactured by SLM.

Numerical approaches were also proposed for the understanding of the residual stress genesis. A first numerical microscopic approach with a 2D geometry of rapid manufacturing process was proposed, see [5], in an early work followed by a macroscopic modelling with a 3D geometry presented in [6] for a similar process, the Direct Metal Deposition (DMD).

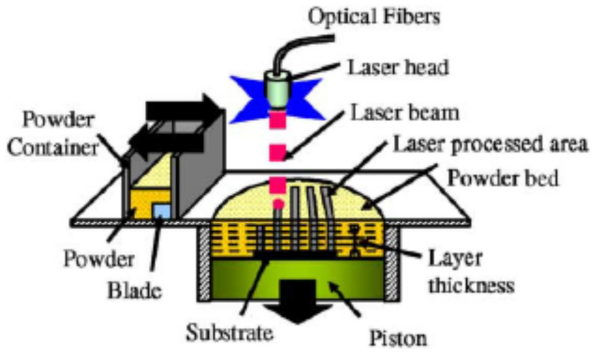

Fig. 1 Schematic illustration of SLM process according to [1]

Related processes like laser powder deposition share the same issue for the prediction of the residual stresses in SLM as found in [7]. Fundamental basis for the transient thermal exchanges are also common with welding, presented in [8] with ABAQUS software.

Numerical model

The issues to address for the numerical modelling of this manufacturing process are close to the simulation of welding but with some different features. The thermal boundary conditions between the solid, the external medium, and the powder are time dependent. The actual physical phenomena involve coupling between transient heat transfers, metallurgical transformation, and mechanical balance of an elastic-plastic material. In the sequel of this paper, only the simple metallurgical phenomenon of annealing is considered, the phase transformation influences are under scrutiny and will be presented in a second paper. In this work, the numerical prediction of the residual stress genesis is conducted with very fine meshes in order to comply with the actual thickness of the powder layer and the actual diameter of the laser spot used in SLM as the stress field is highly dependent of these two geometric parameters. The manufactured parts are parallelepipedic 0.6 mm high, 0.5 mm thick and 0.5 mm large, these small dimensions are chosen in order to bound the computational time to several hours. The input data for ABAQUS Software are automatically generated with an Excel Macro as the birth and death technique of the powder-solidified element needs in this case about 321364 lines of ABAQUS instructions. Such numerical simulations last 107 hours for 3D geometry and 5 hours for 2D geometry and produce a selective results file of 5.21 Go for 3D.

Thermal analysis data

Transient temperature distributions are calculated by solving the heat transfer equations using the finite element method through ABAQUS software. Four nodes elements with reduced integration are used for the meshing of the bed-plate, and a double meshing of the powder layers and the solidified metal, the first one modelling the laid down powder and the second one the manufactured part. This double mesh is associated to an element birth technique for each powder layer laid down followed by an element death technique for the melted powder grain and an element birth technique for the corresponding melted material. With ABAQUS software, the birth of an element is actually its reactivation after a previous “desactivation” following a first meshing [9]. In this model, the solid material has a density ρ of 8,1 g/cm^3, thermal conductivity λ of 21,8 W/m.°C and a specific heat capacity C_p of 440 J/kg.°C at room temperature. The powder thermal properties are deduced

from the mixture law applied to air and the solid material with a powder density of ρ/2 according the energy balance equation. Natural convection is considered on the free surface of the bed-plate whereas natural convection and radiation take place on the free surfaces of the created free surface of the manufactured part and on the upper powder layer. As a first conservative assumption overestimating the residual stresses, perfect contact is assumed between the powder with the bed-plate on the first hand and with the created part on the second hand. These assumptions have to be checked with experimental test of conduction. Once experimental data will be available a mixed boundary condition will be introduced with the actual values of the thermal contact resistance.

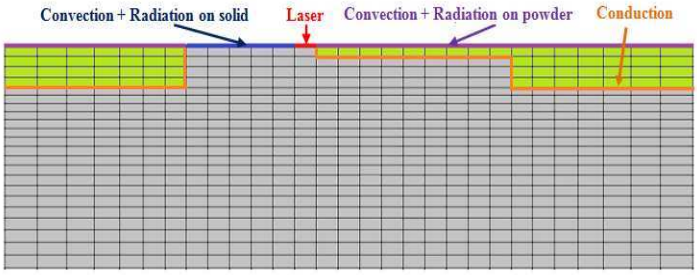

Fig. 2 Mesh and thermal boundary conditions

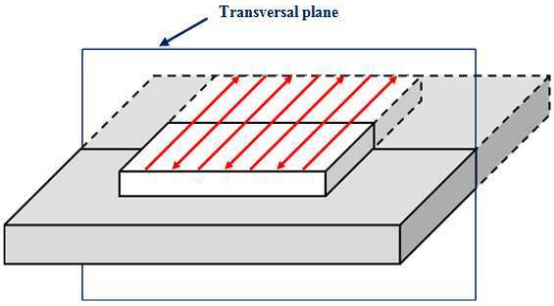

Fig. 3 Cross-section of the part

The heat flux generated by the laser beam is applied to the surface of one element, the size of which is consistent with the actual diameter of the laser spot. The value of the energy density is evaluated at 2000 W/mm^2 following some assumptions about the efficiency of the laser beam and its actual distribution. Ambient temperature is the initial condition for the bed-plate and any powder layer laid down by the machine (Fig. 2). The heating time of the powder element under the laser beam is set to be consistent with the velocity of the laser beam and its path. The 2D model represents the central section of a parallelepipedic part supposed in plane strain state. The same 2D mesh under plane stress condition represents the free surfaces of the same parallelepipedic part perpendicular to the path of the laser beam. The waiting time corresponds to the back and forth moves on the powder layer, see Fig. 3. The size of the mesh of the solidified part and of the powder are chosen in order to comply with the actual thickness of the powder layers, 40 μm, and the effective laser beam diameter, 100 μm.

Mechanical analysis data

For any 3D or 2D models, the mechanical loading comes from the thermal strain distribution. In this particular case, the plastic dissipation is so weak compared to the power of the heat source that the transient heat transfer problem can be solved independently of the internal balance of the elastic-plastic manufactured part. The thermal expansion coefficient is temperature dependent but the effect of any phase transformation is not considered in this first simple model. The bed-plate is considered as simply supported. As no accurate data are available in the temperature range between room temperature and the melting point of the actual material used in the SLM process at PEP, the elastic plastic properties of the 15-5PH steel [10], quite similar to our material, are introduced in the presented numerical simulation (see Fig. 4). The powder is assumed to be a very soft elastic material generating very weak stresses when the layers slide under the effect of the expansion of the manufactured part. The yield stress of the material is very temperature sensitive, at room temperature the yield stress is higher than 800 MPa whence at temperature above 1000°C it is lower than 150 MPa. Data of the Young modulus above 1000°C were not available and an arbitrary minimum value of 2000 MPa is considered for the numerical simulation for temperatures close to the melting point (see Fig. 5). No viscous effects have been introduced in the material behavior, as the cooling times are very short. For the 2D geometry, plane strain, plane stress and generalized plane strain have been considered for the comparison with the 3D case at the level of the residual stress.

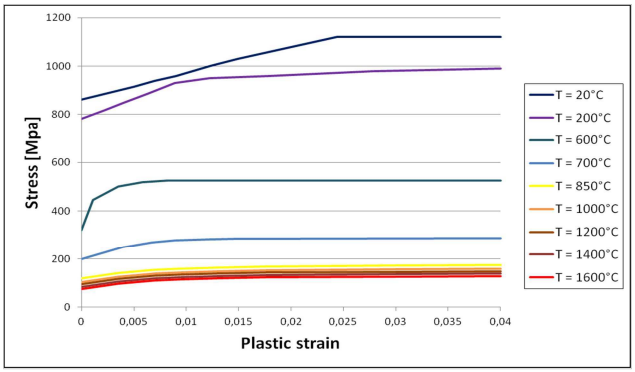

Fig. 4 15-5 PH Hardening curves

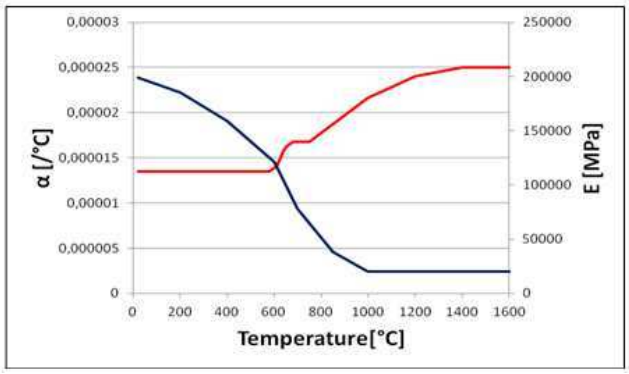

Fig. 5 15-5 PH Young modulus and expansion coefficient

Thermal analysis results

The geometric choices associated with the laser power lead to a maximum temperature close to 1700°C on the surface of the heated element, see Fig. 6. The other peak values of the nodal temperature of an element are reached when its neighbours are heated by the moving laser beam, so a cyclic thermal loading takes place in each element.

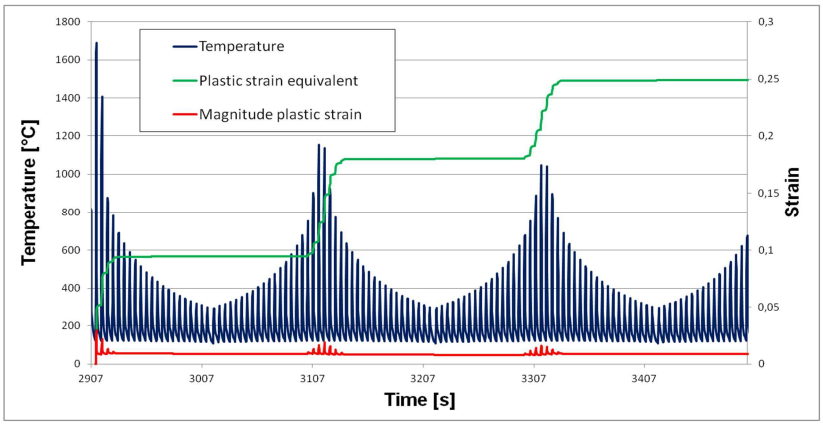

Fig. 6 Thermal and cumulated plastic strain variation in the element at the part centre

The laser beam transforms each melted powder element in a hot sound material clamped by some kind of welding to the colder yet manufactured portion of the part. Under a violent cooling set by the colder existing solidified material the hot new material element shrinks first and its thermal strain is transformed mostly in a tensile plastic strain. Then, as the neighbouring elements close to the new sound element have been heated by the heat flux, they start to cool and their compressive thermal strains are applied to the newly created element deformed once again mostly in its plastic range but with compressive plastic strain. This push-pull kinematics takes place in the created element each time its thermal strain is greater than the maximum elastic strain at the considered temperature. So the thermal loading submits each created elements to a cyclic plastic loading with a cumulative effect on the plastic dissipation evaluated with the cumulated plastic strain, the value of which reaching 25 % after 3 heating cycles when the algebraic plastic strain is less than 1.5 % as tensile and compressive plastic strains are counterbalanced themselves. It is worthwhile to notice for further experimental identification of the metallurgical phenomena that the level of the temperature rate of cooling is close to 5000 °C/s.

Mechanical analysis results

The analysis of the plastic strain distribution with the 3D geometry as the reference shows that the plane strain assumption overestimates the deformation as ε_{33} is constraint to zero. The generalized plane strain condition predicts a good level of cumulated plastic strain but the

distribution does not meet the similar one in any section of the 3D parallelepiped. The plane stress assumption underestimates the level of plastic strain with maximum value equal to 4 % to be compared with the maximum 33 % in the 3D simulation (see Fig. 7).

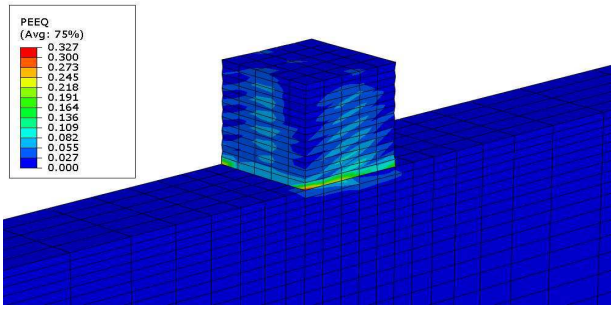

Fig. 7 Cumulated plastic strain in the part 3D

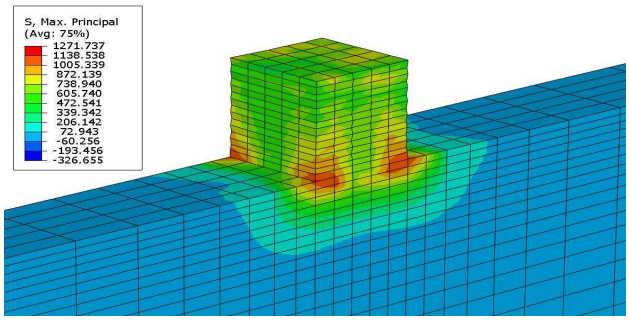

Fig. 8 Maximum principal stress in 3D model

The plane strain and generalized plane strain predict uniform Von Mises stress distribution when the 3D geometry simulation shows high stress level close to 1200 MPa only at the interface between the bed-plate and the solidified part. The four analyzed cases predict high hydrostatic tension at the free corners of the part close to the bed-plate with levels between 500 to 700 MPa. This stress state is dangerous for porous material as hydrostatic tension can initiate damage ahead before crack propagation. The max and min principal stress distribution predicted by plane strain and generalized plane strain assumption are quite similar to the same distribution on the free surface perpendicular to z direction of the 3D parallelepiped where the maximum principal stress values are observed close to 1400 MPa (see Fig. 8). The level of the residual stress is high in the top layer and in the area of the interface between the bedplate. This tendency is in good agreement with experimental results following [4].

Influence of the annealing temperature

As a first metallurgical parameter, the influence of the annealing temperature of the material is analysed. Under the effect of the laser beam, high temperatures in the melted powder are reached in few seconds. Existing data on the annealing temperature corresponds to heating lasting several hours. As no reliable data is available in the literature for the heating time under consideration for SLM, the values of this important parameter governing the cancellation of the plastic strain have been chosen arbitrarily close to the melting point. As presented at Fig. 9, the cumulated plastic strain reached during the first heating of an element, for example at 2900 seconds, can be cancelled by further heating coming from its neighbouring elements, with this cancellation controlled by the actual annealing temperature at 3100 and 3300 seconds. The cumulated plastic strains continuously increase as long as the annealing phenomenon is not activated. With an annealing temperature equal to the melt temperature, the maximum cumulated plastic strain is equal to 40% whereas with an unrealistic arbitrary value of 1000°C, the maximum cumulated plastic strain is less than 25 %.

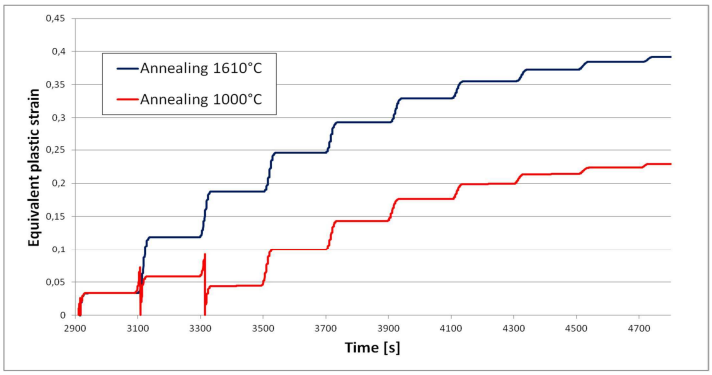

Fig. 9 Cumulated plastic strain for annealing

This difference is important for the final level of the residual stress if the material is sensitive to plastic strain hardening. Actually, this issue is also connected to the actual behaviour of the material under hardening. This first numerical model of SLM assumed an isotropic hardening but kinematic hardening and mixed hardening have to be investigated too in further works.

Summary

For further numerical simulations of SLM process with actual geometric parameters, this work shows that generalized plane strain analysis can predict realistic stress distributions on a parallelepiped's free surface perpendicular to the laser beam displacement where failure are observed. In order to analyse the influence of metallurgical phenomena on the residual stress, 2D analysis with generalized plane strain condition seems to be convenient as they are not very CPU time consuming but for any optimization of the manufacturing process, 3D analysis remains absolutely necessary.

References

[1] E.C. Santos, M. Shiomi, K. Osakada, T. Laoui, Rapid manufacturing of metal components by laser forming, International Journal of Machine Tools & Manufacture 46 (2006) 1459-1468.

[2] C. Casavola, S.L. Campanelli, C. Pappalettere, Experimental analysis of residual stresses in the Selective Laser Melting process, Proccedings of the XIth International Congress and Exposition, Orlando, Florida, USA, June 2-5, 2008.

[3] J.-P. Kruth, M. Badrossamay, E. Yasa, J. Deckers, L. Thijs, J. Van Humbeeck, Part and material properties in Selective Laser Melting of metals.

[4] M. Shiomi, K. Osakada, K. Nakamura, T. Yamashita, F. Abe, Residual stress within metallic model made by Selective Laser Melting process.

[5] M. Shiomi, A. Yoshidome, F. Abe, K. Osakada, Finite element analysis of melting and solidifying processes in laser rapid prototyping of metallic powders, International Journal of Machine Tools & Manufacture 39 (1999).

[6] A. Longuet, C. Colin, P. Peyre, S. Quilici, G. Cailletaud, Modélisation de la fabrication directe de pièces par projection laser : application au Ti-6Al-4V, Matériaux, novembre 2006.

[7] C.S. Zhang, L. Li, A. Deceuster, Thermomechanical analysis of multi-bead pulsed laser powder deposition of a nickel-based superalloy, Journal of Materials Processing Technology 211 (2011) 1478-1487.

[8] J. Ding, P. Colegrove, J. Mehnen, S. Ganguly, P.M. Sequeira Almeida, F. Wang, S. Williams, Thermo-mechanical analysis of Wire and Arc Additive Layer Manufacturing process on large multi-layer parts, Computational Materials Science, 2011.

[9] A. Pilipenko, Computer simulation of residual stress and distortion of thick plates in multi-electrode submerged arc welding. Thesis, July 2001.

[10] T. Wu, Experimental and numerical simulation of welding induced damage, stainless steel 15-5PH, Thesis, 2007.

Material Forming ESAFORM 2012
10.4028/www.scientific.net/KEM.504-506

Comparisons of Numerical Modelling of the Selective Laser Melting

10.4028/www.scientific.net/KEM.504-506.1067